Array Processing of Flow Noise

By

P E Madden and S G Wright

AUWE, Portland

Introduction

The sonar performance of a homing torpedo is limited by self noise. Flow noise is an important contributor and is inevitable if the flow becomes turbulent since the pressure fluctuations produce a source of sound which can be heard by detectors designed to receive acoustic energy. This paper is concerned with the response of an array of sensors positioned on the flat at the front of a torpedo nose. Because of the security classification of the array operating frequency, this is referred to as f_0 and all other frequencies are relative.

The first slide (Figure 1) shows the situation which is being studied. The noise results from the turbulent part of the flow and its location can be found by using the techniques of flow visualisation. This slide (Figure 2) shows the nose unit which has been painted with a mixture of paraffin and fluorescent dye, and then run in a wind tunnel at the appropriate Reynolds number, thus correctly modelling the flow. Over the forward part of the nose there is laminar flow which does not dry the paraffin very quickly and the dye does not fluoresce under ultra-violet light. Turbulent flow is more effective at drying the liquid. The paraffin therefore evaporates leaving the dry dye which does fluoresce under ultra-violet light. The photograph shows this as a lighter region and indicates the area of turbulence. It is this area which is the source of flow noise.

The energy travels to the array via the structure and water. In this nose unit the structure dominates. The nose was placed on the front of the AUWE test vehicle and run such that the only significant source of noise was that due to flow over the nose with no cavitation present. The data were recorded on a Honeywell 5600 tape recorder carried in the vehicle.

There are several ways in which the processing of the array could be studied. Firstly, if we take the mechanism of flow noise just described, it should be possible to calculate the response of the array and hence understand the processing. This does not turn out to be possible in practice because there are too many difficulties associated with the different types of structural waves and the diffraction around the edge of the body, which makes the mathematical analysis extremely complex. To simplify the calculations somewhat, one could measure the response of the elements by placing an acoustic source at the point of the flow transition and rotating it around the body. This establishes the amplitude response of the element to a flow noise source but does not give any information on the all important relative phases which are in turn associated with the velocities of the different waves travelling from the source to the array. It turns out that this approach does not predict the array response with sufficient accuracy.

The final approach overcomes the difficulties of calculating propagation through the media which carry the energy by measuring the output from the elements themselves. This amounts to study of the array alone, and the

mechanisms which carry the energy from the turbulent boundary layer can be studied separately. This reduces the problem to one of predicting the beam outputs from the known responses of individual elements and thereby enables the system to be optimised.

Array and Beam Forming

The next slide (Figure 3) shows the array that was used on the front of the torpedo nose. There are 55 elements in the array but recording all of these outputs is not convenient within a torpedo sized body. The tape recorder which was used had only 14 data channels, 7 on each of the 2 recording heads and this limited the number which could subsequently be analysed to give cross-correlation and cross-spectra. The 7 elements which were recorded are taken from the same area of the array and are numbered in the slide. Additionally, they were formed into 2 sub-beams (Figure 4). One of these sub-beams was unsteered and unshaded - the 7 element outputs being summed and recorded on the other head simultaneously with the element outputs. The other sub-beam, although still unshaded, was steered to an angle of 45°. This angle was not especially chosen except to be significantly different from the unsteered beam. It resulted from the type of steering that was used where adjacent elements were phase shifted by 90° at the resonant frequency of the array. These phased element outputs were then summed and recorded on to the other tape recorder head.

For earlier runs it was not completely proven that cross-correlations and cross-spectra could be measured from the tape recorder and therefore it was decided to carry out some restricted processing on board the test vehicle. The slide (Figure 5) shows the electronics which were used and the multiplexing time was chosen so that all combinations of element multiplication were recorded in 18 seconds. The filters were interchangeable and 3 sets had bandwidths of 200 Hz, 1 KHz and 6 KHz. The output was rectified and smoothed and recorded on the tape recorder.

An example of the output from this multiplex system is shown in the next slide (Figure 6). The bandwidth for the filter is 6 KHz. The large responses are the auto-correlations and the different amplitudes show that the energy is not equally distributed over the array. Between these large spikes are the cross-correlation terms and it is clear that these are small and therefore will not figure to any significant extent in the array processing. These results, and others are similar, were compared with measurements using the tape recorder data. There was agreement which showed that the tape recorder data could be used to carry out the study.

Array Processing

Here (Figure 7) we see examples of the spectra of outputs that were recorded during a run. The sub-beam outputs do not follow exactly the shape of the single element curves because the outputs are dependent on more than energy alone. What is required is to take this basic element information and predict the sub-beam outputs in these particular cases. If that is possible, then in principle we can compute the beam outputs for any frequency, steer angle and shading and then optimise the system which we have.

Let us consider first a simple case where the noise is not correlated between elements and has an equal amplitude over the array. Then the noise power in the array is proportional to the number of elements N and the signal power is expected to vary as N^2 because in this case the correlation coefficient between the elements is unity. This gives a signal to noice ratio of 10 log N dB

and this is a well known result. However, it has already been shown that flow noise is partially correlated between the elements and the amplitude distribution is not uniform. It is therefore not appropriate to consider this simple model. For positive values of the correlation, signal to noise ratio will worsen, but in favourable circumstances, the values of the correlation may be negative and lead to a cancellation of noise across the array. By building up a picture of the correlation structure, an array amplitude shading may be developed to take advantage of any negative values of the correlation and any distribution of power across the array. In a similar way the effects of beam steering may be calculated by finding the change in correlation with applied time delay or phase shift. Moving from the time domain to the frequency domain, correlation analysis is replaced by a spectrum analysis but the method is essentially the same.

In general, the noise will be partially correlated between elements, and noise will be summed in the array as shown in this slide (Figure 8). Looking first at the time domain, the noise voltage $n_i(t)$ at the i^{th} element is multiplied by a shading coefficient x_i and summed with the other elements of the array - equation 1. To find the mean power in the array, the output is squared and averaged over a length of time, giving the double sum shown in equation 2. Flow noise will be shown below to be stationary, so for a suitably long averaging time the array power level is given by the double sum of correlation values for zero time delay, $A_{ik}(0)$, multiplied by the shading terms - equation 3. On beam-steering, each element output will be delayed by a length of time. In general the relative time delay between the i^{th} and k^{th} elements will be τ_{ik}, so the relevant terms in the double sum will be $A_{ik}(\tau_{ik})$, giving equation 4.

In the frequency domain the noise at the i^{th} element at frequency f will be given by the complex quantity $N_i(jf)$. A similar series of equations is gone through as for the time domain, the cross-correlation being replaced by the cross-spectrum $S_{ik}(jf)$. The imaginary parts of the cross-spectrum sum to zero, giving the straight beam output of equation 5. On steering the phase ϕ_{ik} of the cross-spectrum is modified by the relative applied steering phase ϕ_{sik}, and the steered beam output is given by equation 6. Normalising the correlation or cross-spectrum matrix to the centre element gives the "flow-noise matrix" as defined in the next slide (Figure 9). Normalising to the diagonal terms of the matrix gives the correlation coefficients or "cross-spectrum coefficients"; these terms show the similarity between noise at 2 elements for a particular time shift or phase shift. In the frequency domain the coherence is also used; by using the modulus of the cross-spectrum the coherence shows the similarity between the noise at 2 elements irrespective of the phase of the cross-spectrum or of the applied steering phase.

In the time domain therefore we need to consider the correlation between elements. The slide (Figure 10) shows how this varies with time delay for 2 pairs of elements taken from the sub-array at the frequency f_0. The outputs are always displaced sinusoids and the amplitude does not decay significantly over a number of cycles even for the widest band of 6 KHz. In fact the results are bandwidth independent over the range considered. From these outputs the correlation can be read directly for the unsteered and steered beams. In the case of the unsteered beam we look at the correlation for zero time delay. For the steered beam we have to look at the appropriate time delay between the elements. For some cases this will mean that we use the value at a finite delay but if the elements are not delayed with respect to each other, the steered value will be the same as that for the unsteered case.

Flow noise is a stationary process and the results are repeatable. This slide (Figure 11) shows the relationship between element pairs measured on 3 runs for the same nose unit. The next slide (Figure 12) shows how the correlation between a pair of elements varies with time during the run. The mean remains constant throughout and the variations about this mean are consistent with the bandwidth and smoothing used to make the record. Therefore the correlation or flow noise matrix can be constructed for both the steered and unsteered beams. We can see (Figure 13) in both of these cases that the leading diagonal which represents the energy distribution across the array is the same but the off diagonal terms are generally different and at this frequency are small. To compute the beam outputs, it is simply a matter of adding together all the terms in the matrix. It is seen (Figure 14) that the agreement between the measured and the calculated outputs is good and therefore we have got confidence in applying this technique to find the beam outputs at other angles of steer which we did not measure. This is done from the correlation/time plots shown previously. For a particular angle of steer the appropriate relations are measured and the beam output calculated at that steer angle. The result (Figure 15) is that we can plot the steered to straight beam ratio as a function of the angle of steer and the slide shows that at this particular frequency, there is not very much variation, even up to angles as large as 90°. The reason for this is that the correlation is always small for the off diagonal terms irrespective of time delay. If we want to calculate an optimised shading pattern for this particular beam output, this is most conveniently done by using the standard techniques of linear programming. An algorithm (Figure 16) was written by Nottingham University based on the method of Beale which minimises this quadratic function subject to constraints. For the flow noise problem, the first term is not needed. and the constraint imposed is that the sum of the shading coefficients must be constant. This is equivalent to maximising the signal to noise ratio.

The result (Figure 17) of this optimisation shows little difference between that and unity shading. The reasons for this are twofold. Firstly, the off-diagonal terms are small and therefore the shading pattern when multiplied by these terms does not significantly modify the output. Secondly, the distribution of energy along the leading diagonal is not very great. Therefore, there is little difference between shading patterns on the signal to noise output at this frequency and the shading pattern would therefore be chosen with other factors in mind eg low side lobes. In fact a low side lobe shading would be almost optimum in this case because the noise output tends to increase towards the outer edge of the array whereas a low side lobe shading would have a taper in the opposite direction therefore tending to make noise outputs equal which in the absence of the off-diagonal terms would be optimum.

If we look at the coherence (Figure 18) between a pair of elements, it shows that at the frequency f_0 the value is low. This we would have expected because the off-diagonal correlation terms have been shown to be small. However, the coherence is not low at all frequencies and in particular it is high at the frequency f_0-5 KHz. In this region we would expect that the off-diagonal correlations would be large and therefore beam outputs would be significantly affected by shading and steering. In order to study the beam processing at this frequency we could repeat the procedure used at f_0 where we work in the time domain. However, this would require the building of filters at this frequency. This is not necessary if we work in the frequency domain and look at the cross-spectra between the various element pairs. The theory has shown that there is a duality between these 2 approaches and

if we look at the cross-spectrum for a typical pair of elements, we obtain real and imaginary parts as a function of frequency. To form the flow noise matrix from this information is particularly easy for the 2 sub-beams under consideration. For elements which have no phase difference it is appropriate to take only the real part of the cross-spectrum. If the elements have a phase difference of 90°, then one takes only the imaginary part of the cross-spectrum. Therefore in this way the 2 flow noise matrices can be constructed. The difference between these matrices and those at the frequency f_0 are apparent on 2 counts (Figure 19). Firstly, there is a much greater difference in energies across the array as shown by the leading diagonal, and secondly, the off-diagonal terms are of comparable magnitude. Therefore we would expect that optimising the shading would significantly improve the signal to noise ratio. This is indeed the case as the slide (Figure 20) shows. and when these shading factors are applied to the element outputs from the tape recorder, the resultant improvement in the signal to noise output compared with unity shading is more than 8 dB. Calculating the flow noise matrices for the 2 sub-beams considered was especially easy since either real or imaginary parts were the only ones to be considered. However, if an appropriate vector addition of the 2 components is made, it is possible to calculate the flow noise matrix for any steer angle and the slide (Figure 21) shows the result. We find in this case that steered beams are less noisy than unsteered beams which is contrary to the result at f_0 and we find that the variation with steer angle is in excess of 20 dB compared with about 2 dB. This is a direct result of the large off-diagonal terms.

Conclusions

This work has shown that flow noise is a stationary process with consistent levels from run to run. Therefore it is not necessary to have an adaptive processing system; the array can be studied at the design stage and an optimised shading can be introduced. For this nose unit, coherence was small at the resonant frequency of the array and therefore array shading and steering did not considerably modify the beam outputs. However, it was shown that the coherence at other frequencies was large and an optimised shading was chosen to reduce the noise output by 8 dB. Steering the beam also had a considerable effect. Therefore the resonant frequency of the array might not be the one which gives the highest signal to noise output. Careful considerations need to be made to choose the best frequency to be used for a particular application. The technique described in this paper can be used to choose this frequency.

Application to large arrays has obvious difficulties - the main one being the size of the flow noise matrix. Symmetry in the array eliminates the need to measure all element pairs and therefore the total number of combinations is considerably reduced. However, several runs will probably be required to gather all of the data.

Development of torpedo noses is still continuing and changes in shape and constructions are expected to increase the correlations at the resonant frequency. But using the techniques which have been described here, it will still be necessary to optimise the system for the particular set of circumstances which will be encountered.

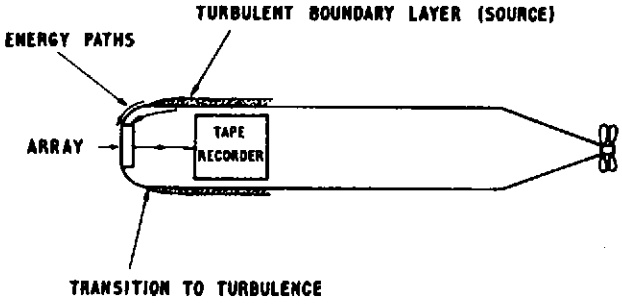

FIG 1 FLOW NOISE PROCESS

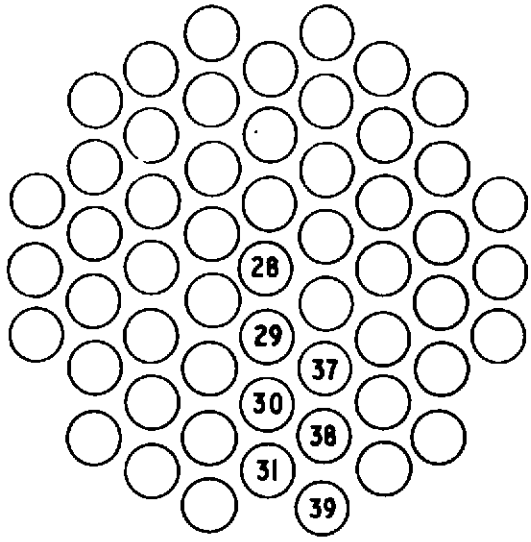

FIG 3 ARRAY

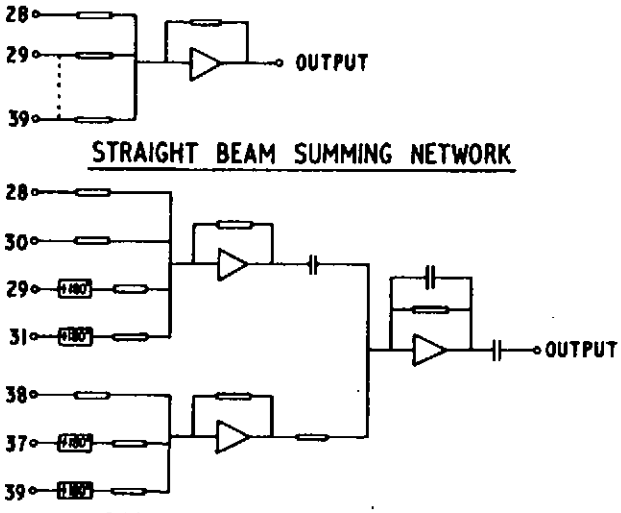

FIG 4 STEERED BEAM SUMMING NETWORK

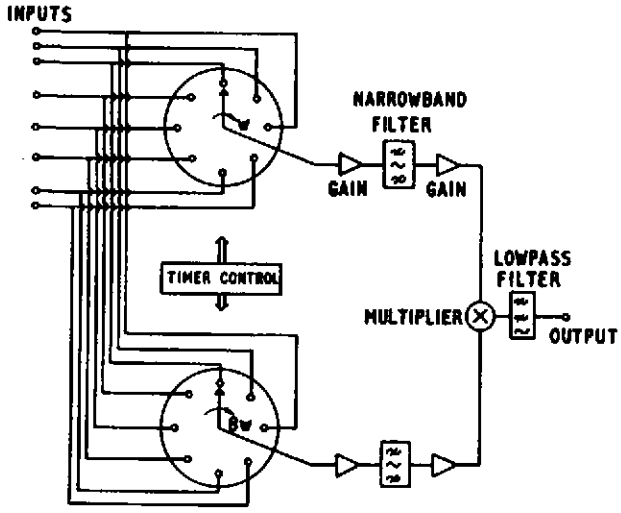

FIG 5 MULTIPLEXER ELECTRONICS

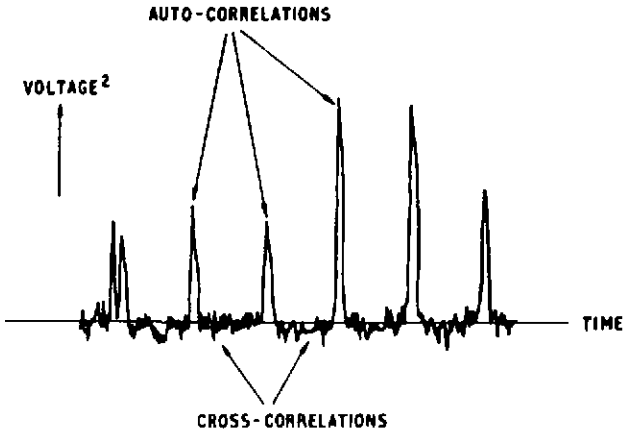

FIG 6 OUTPUT FROM MULTIPLEXER

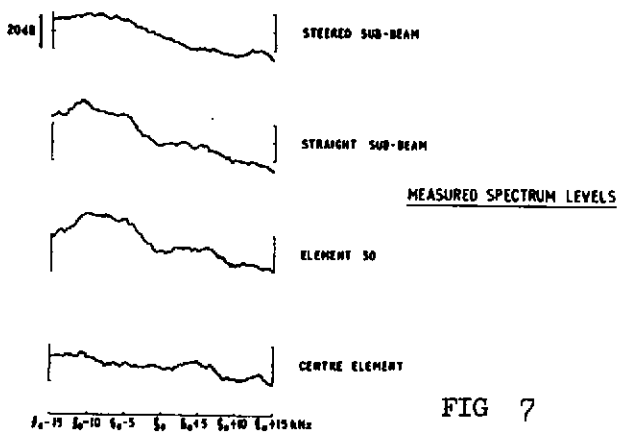

FIG 7

TIME DOMAIN	FREQUENCY DOMAIN
STRAIGHT BEAM SUMMATION	
$v(t) = \sum_{i=1}^{N} x_i a_i(t)$ (1)	$v(jf) = \sum_{i=1}^{N} x_i a_i(jf)$
$\overline{v^2(t)} = \sum_{i=1}^{N}\sum_{k=1}^{N} x_i x_k \overline{a_i(t) a_k(t)}$ (2)	$v(jf)v^*(jf) = \sum_{i=1}^{N}\sum_{k=1}^{N} x_i x_k a_i(jf) a_k^*(jf)$ $= \sum_{i=1}^{N}\sum_{k=1}^{N} x_i x_k S_{ik}(jf)$
	IMAGINARY PARTS SUM TO ZERO ∴
$\overline{v^2(t)} = \sum_{i=1}^{N}\sum_{k=1}^{N} x_i x_k A_{ik}(0)$ (3)	$v(jf)v^*(jf) = \sum_{i=1}^{N}\sum_{k=1}^{N} x_i x_k \lvert S_{ik}(jf)\rvert \cos(\phi_{ik})$ (5)
WHERE $A_{ik}(0)$ = CROSS-CORRELATION FOR ZERO TIME DELAY	WHERE $S_{ik}(jf) = \lvert S_{ik}(jf)\rvert e^{j\phi_{ik}}$ = CROSS-SPECTUM
STEERED BEAM SUMMATION	
ARRAY OUTPUT $= \sum_{i=1}^{N}\sum_{k=1}^{N} x_i x_k A_{ik}(\tau_{ik})$ (4)	ARRAY OUTPUT $= \sum_{i=1}^{N}\sum_{k=1}^{N} x_i x_k \lvert S_{ik}(jf)\rvert \cos(\phi_{ik} + \theta_{Sik})$ (6)

FIG 8 TIME AND FREQUENCY DOMAIN ANALYSIS

TIME DOMAIN	FREQUENCY DOMAIN
COMPONENT OF FLOW-NOISE MATRIX $A_{ik}(\tau_{ik}) / A_{ii}(0)$	COMPONENT OF FLOW-NOISE MATRIX $\lvert S_{ik}(jf)\rvert \cos(\phi_{ik} + \theta_{Sik}) / S_{ii}(jf)$
CORRELATION COEFFICIENT $= A_{ik}(\tau_{ik}) / [A_{ii}(0) A_{kk}(0)]^{\frac{1}{2}}$	"CROSS-SPECTRUM COEFFICIENT" $= \lvert S_{ik}(jf)\rvert \cos(\phi_{ik} + \theta_{Sik}) / [S_{ii}(jf) S_{kk}(jf)]^{\frac{1}{2}}$
	COHERENCE $= \lvert S_{ik}(jf)\rvert^2 / S_{ii}(jf) S_{kk}(jf)$

FIG 9 FORMATION OF THE FLOW-NOISE MATRIX

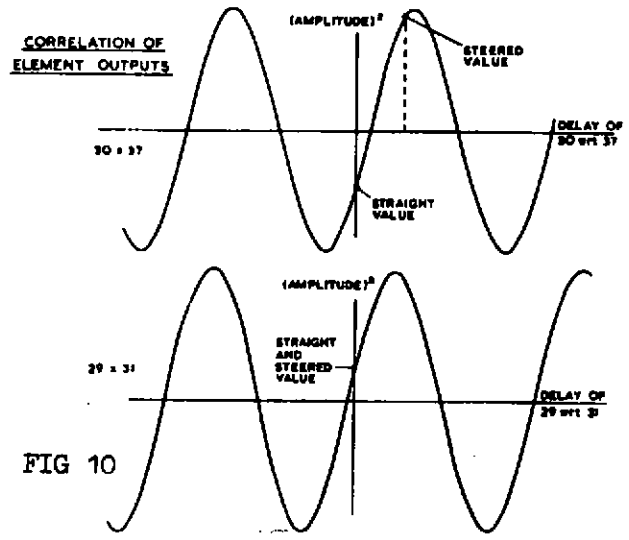

FIG 10

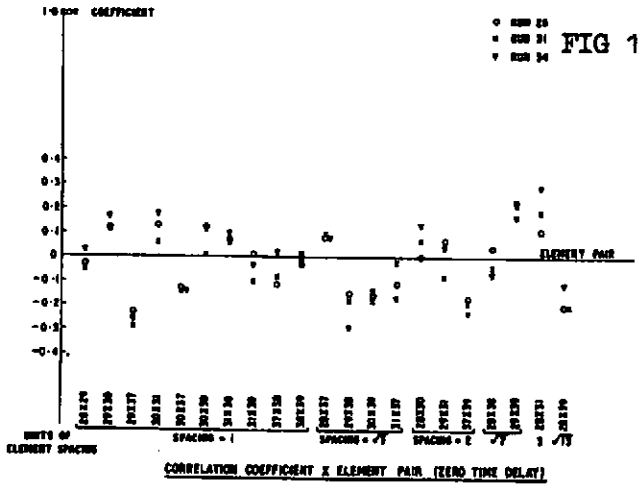

FIG 11

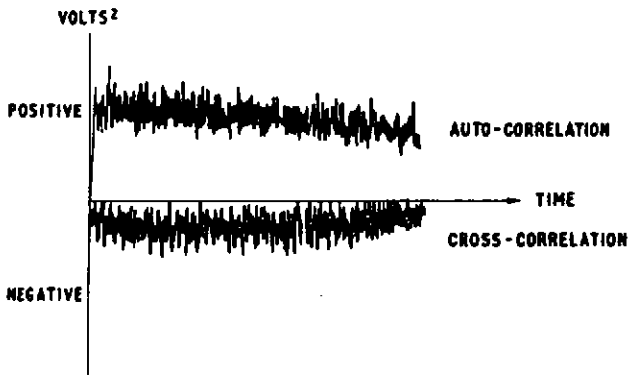

FIG 12 VARIATION OF CORRELATION WITH TIME

	28	29	30	31	37	38	39
28	1·0	·04	0	·24	·09	·07	·39
29	·04	1·52	·16	·19	·33	·32	·55
30	0	·16	1·18	·33	·16	·23	·34
31	·24	·19	·33	5·10	·29	·29	·04
37	·09	·33	·16	·29	1·37	·24	·40
38	·07	·32	·23	·29	·24	3·19	·11
39	·39	·55	·34	·04	·40	·11	3·92

STRAIGHT FLOW-NOISE MATRIX - S_{ik}

	28	29	30	31	37	38	39
28	1·0	·02	0	·24	·08	·18	·34
29	·02	1·52	·20	·19	·33	·19	·39
30	0	·20	1·18	·37	·42	·26	·21
31	·24	·19	·37	5·10	·37	·28	·11
37	·08	·33	·42	·37	1·37	·27	·40
38	·18	·19	·24	·28	·27	3·19	·14
39	·34	·39	·21	·11	·40	·14	3·92

FIG 13 STEERED FLOW-NOISE MATRIX - S_{ik}

STEERED SUB-BEAM LEVELS: MEASURED (dB) x PREDICTED (dB)

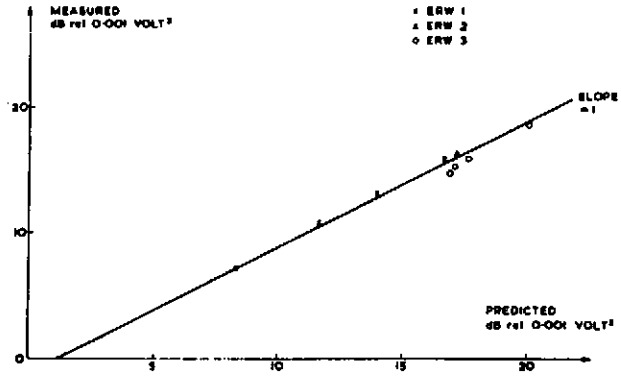

FIG 14

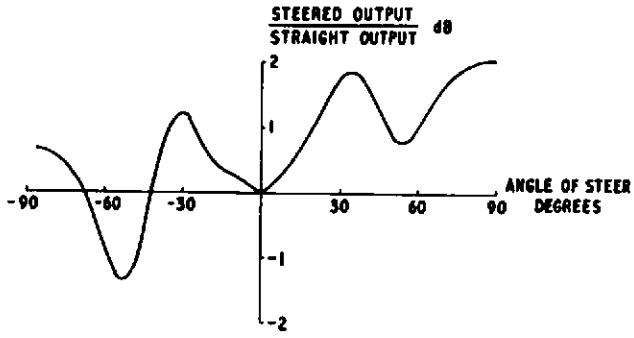

FIG 15 CALCULATED RESPONSE OF STEERED BEAM AT f_0

OPTIMIZATION PROGRAM

FIND THE Xi's TO MINIMISE THE FUNCTION

$$Z = \sum_{i=1}^{N} Ci\ Xi + \sum_{i=1}^{N} \sum_{\substack{k=1 \\ i<k}}^{N} Cik\ Xi\ Xk + \sum_{i=1}^{N} Cii\ Xi^2$$

SUBJECT TO A SET OF CONSTRAINTS OF THE TYPE

$$\sum_{i=1}^{N} Ai\ Xi = B \qquad \text{WHERE } B \text{ AND } Xi \geq 0$$

APPLICATION TO FLOW NOISE

FOR Ci = 0 AND Aik = Aki = Cik/2, FUNCTION TO BE MINIMISED IS

$$Y = \sum_{i=1}^{N} \sum_{k=1}^{N} Aik\ Xi\ Xk$$

ARRAY OUTPUT TO BE MINIMISED — FLOW NOISE MATRIX — ARRAY SHADING TO BE FOUND

SUBJECT TO THE CONSTRAINT $\sum_{i=1}^{N} Xi = N$

THIS IS EQUIVALENT TO MINIMISING THE NOISE/SIGNAL POWER RATIO $\frac{1}{S}$ SINCE

$$\frac{1}{S} = \frac{\sum\sum Aik\ Xi\ Xk}{\sum\sum Bik\ Xi\ Xk} \qquad \text{AND } Bik = 1$$

$$\therefore \frac{1}{S} = \frac{\sum\sum Aik\ Xi\ Xk}{(\sum Xi)^2}$$

FIG 16 SHADING OPTIMIZATION

FIG 17

FLOW-NOISE MATRIX

1·0	$\bar{0}$·04	0·0	·24	·09	·07	$\bar{3}$9
	1·52	·16	·19	$\bar{3}$3	$\bar{3}$2	·55
		1·18	·33	$\bar{1}$6	·23	$\bar{3}$4
			5·10	$\bar{2}$9	·29	·04
				1·37	$\bar{2}$4	$\bar{4}$0
					3·19	$\bar{1}$1
						3·92

SHADING VECTOR

1·5
1·1
1·3
0·1
1·7
0·6
0·7

10 LOG $\left(\frac{\text{OPTIMIZED POWER}}{\text{UNITY POWER}}\right)$ = 2·1 dB

OPTIMIZATION RESULTS AT f_0

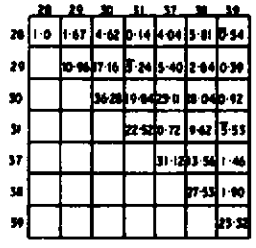

STRAIGHT FLOW-NOISE MATRIX AT f_0-5kHz

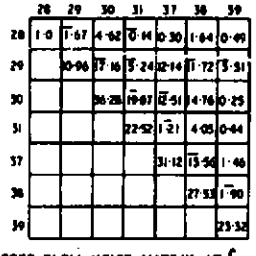

STEERED FLOW-NOISE MATRIX AT f_0-5kHz

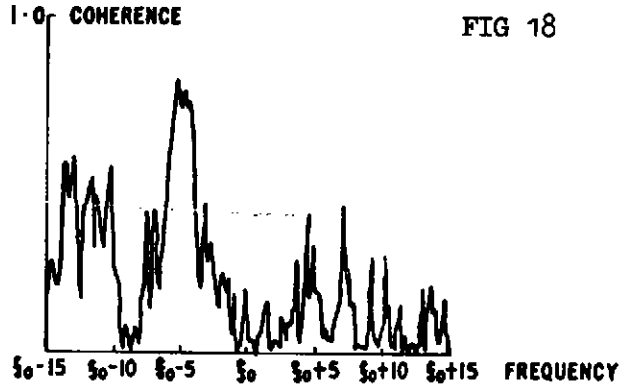

FIG 18

COHERENCE BETWEEN ELEMENTS 28 AND 29

FIG 19

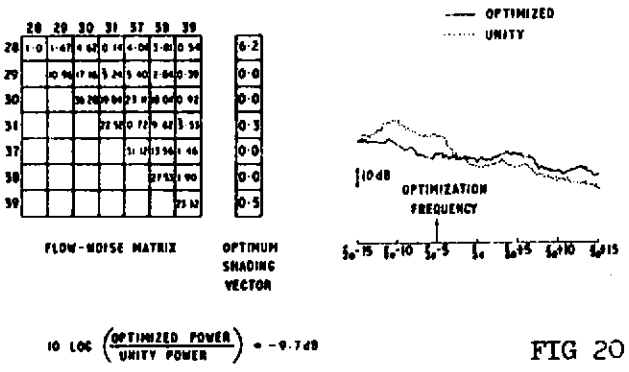

FIG 20

STRAIGHT SUB-BEAM SHADING OPTIMIZATION AT f_0 - 5kHz

FIG 21

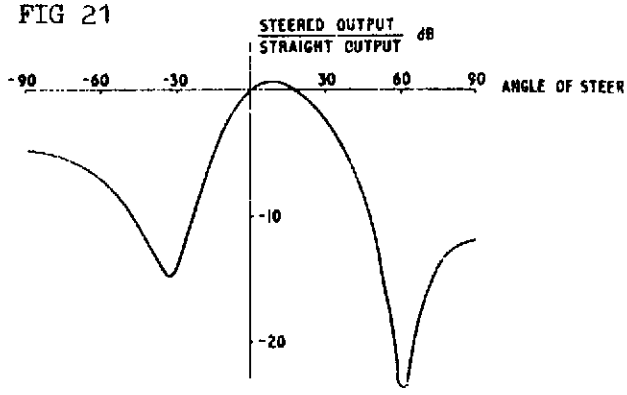

CALCULATED RESPONSE OF STEERED BEAM AT f_0 - 5kHz